 CMES, vol.12, no.2, pp.149-157, 2006

Spectral Element Approach for Forward Models of 3D Layered Pavement

Chun-Ying Wu[1,3], Xue-Yan Liu[2], A. Scarpas[2], and Xiu-Run Ge[3]

Abstract: For the spectral analysis of the three-dimensional multi-layered pavement, 3D layer spectral element method is presented to solve the problems of bounded layer system subjected to a transient load pulse. In spectral element, each layer is treated as one spectral element. The wave propagation inside each layer element is achieved by the superposition of the incident wave and the reflection wave. Fast Fourier transformation is used to transform FWD datum from time domain to frequency domain. The accuracy and efficiency of 3D layer spectral element approach were verified by analyzing the Falling weight deflectometer(FWD) testing model with the spectral methods and the finite element method(FEM).

keyword: 3D layer spectral element, Falling weight deflectometer, Fast Fourier transformation

1 Introduction

Both the analytical and numerical methods have been extensively applied into solving dynamic problem ranging from seismic wave propagation, soil-structure interaction by vibrations, fluid-solid interface wave propagation, as well as non-destruction testing problem. Falling weight deflectometer(FWD) is a non-destructive dynamic method widely used for the evaluation of pavement structures. Most of the parameter identification computer programs used today for analyzing FWD datum are based on the static analysis, which often underestimates the strength of pavement subgrade. However, when applying dynamic analysis for FWD study, the computational efficiency is always a big concern in the parameter identification of inverse calculation. For instance, Lee(1998) employed two-dimensional, dynamic finite element analysis using the ABAQUS program to develop the deflection information for the FWD study. Bozkurt(2002) reconstructed 3-D finite element meshes to analyze the airport pavement. It is known that finite element method, an effective numerical method, can be commonly used to analyze complicated models with different geometries and loading conditions. However, it is not efficient in the forward and inverse calculation due to discrete characteristics of element meshes. On the other hand, analytical dynamic method, though very efficient, is usually cumbersome for the models with complicated geometries and boundary conditions. Therefore, semi-analytical dynamic method was proposed by the combination of the analytical solution in solids with the numerical technique of finite element. Thomson(1950) and Haskell(1953) developed a propagator approach, in which a propagator matrix combined with the known displacements and forces can be transferred from one interface to another. However, because the transforming matrix is nonsymmetrical, this method is still not efficient in the numerical calculation. Besides the efficiency, the propagator approach has difficulty in dealing with different boundary conditions. Kausel and Roesset(1981) modified the propagator matrix to a symmetric transforming matrix by a series of function transforms corresponding to different boundary conditions. Due to the complicated transforms, the time consumption for the calculation still remains a problem.

Spectral element method as one of the semi-analytical methods was developed by Doyle, which describes waveguides in the element as the superposition of incident waves and reflection waves. Following the theory, Doyle(1997) applied spectral analysis mainly for the 1-D waveguide, Rizzi(1992) focused the work on the response of the wave propagation in 2-D layered solids, and Al-Khoury(2001) utilized the spectral element to analyze the dynamic impact of FWD load pulses on pavements. On the basis of this forward model, an inverse calculation by use of three minimization algorithms was presented for the parameter identification of FWD datum. Yongon(1998) employed Hankel transforms as a forward model and an artificial neural network (ANN) for the in-

[1] Highways Engineering Research Department, Jiangsu Transportation Research Institute, Nanjing, P.R. China
[2] Section of Structural Mechanics, Faculty of Civil Engineering and Geosciences, Delft University of Technology, Delft, Netherlands
[3] Department of Civil Engineering, Shanghai Jiaotong University, Shanghai, P.R.China, wu_chunying@sjtu.edu.cn

version process. However, previous work only solved problems in the 2-D or the semi-infinite multi-layered system.

The objective of this study is to develop a new type of spectral element for three-dimensional layer system. The 3-D layer spectral element and the throw-off spectral element are presented in the study. The stiffness matrix for every element is derived by the exact solution of wave propagation in structure. The formula of Lamb(1904) are applied for wave propagating solution in three-dimensional solids. Thus, this method can be used to solving more complicated dynamic problems such as the pavements subjected to the FWD loading.

2 Governing Equations

When homogeneous isotropic elastic solid with constant elastic material is subjected to dynamic loads, two types of waves are generated: dilatational (P) wave and shear (S) wave. Assuming the symmetry on the axis of z, the equation of wave propagation for a three-dimensional element holds

$$\mu\Delta u+(\lambda+\mu)\nabla(\nabla\cdot u)=\rho\frac{\partial^2 u}{\partial t^2} \tag{1a}$$

$$\Delta u=\nabla(\nabla\cdot u)-\nabla\times(\nabla\times\vec{u}) \tag{1b}$$

where $u=\{u(x,y,z,t),v(x,y,z,t),w(x,y,z,t)\}$is the displacement, ρ is the mass density, λ and μ are the Lame's constants.

$$\lambda=\frac{\nu E}{(1+\nu)(1-2\nu)},\quad \text{and } \mu=\frac{E}{2(1+\nu)} \tag{2}$$

E is Young's modulus and νis Poisson's ratio. $\nabla=x_0\frac{\partial}{\partial x}+y_0\frac{\partial}{\partial y}+z_0\frac{\partial}{\partial z}$ is set as an operator, $\Delta=(\nabla\cdot\nabla)=\frac{\partial^2}{\partial x^2}+\frac{\partial^2}{\partial y^2}+\frac{\partial^2}{\partial z^2}$ is the Laplacian operator. $(\cdot)$ and $(\times)$ are scalar and vector products , respectively.

The displacement vectors are composed as the sum of the gradient of a scalar potential φ and the curl of a vector potential ψ,

$$u=\nabla\varphi+\nabla\times\psi,\quad \nabla\cdot\psi=0 \tag{3}$$

where φ is related to dilatational wave and ψ is related to shear wave.

From the article of Lamb(1904), the formula of displacement are expressed by two potentials as below,

$$u=\frac{\partial\varphi}{\partial x}+\frac{\partial^2\psi}{\partial x\partial z},v=\frac{\partial\varphi}{\partial y}+\frac{\partial^2\psi}{\partial y\partial z}, \tag{4}$$

The potentials φ and ψ are written as dynamic equations,

$$\Delta\varphi=\frac{1}{C_p^2}\frac{\partial^2\varphi}{\partial t^2} \tag{5a}$$

$$\Delta\psi=\frac{1}{C_s^2}\frac{\partial^2\psi}{\partial t^2} \tag{5b}$$

with $C_p=\sqrt{(\lambda+2\mu)/\rho}$, $C_s=\sqrt{\mu/\rho}$

Here, C_p andC_s are the wave velocities of P and S waves. The relevant stresses expressed by potentials φ and ψ hold

$$\sigma_{zx}=2\mu(\frac{\partial^2\varphi}{\partial x\partial z}+\frac{\partial^3\psi}{\partial x\partial z^2})-\rho\frac{\partial^3\psi}{\partial x\partial t^2} \tag{6a}$$

$$\sigma_{zy}=2\mu(\frac{\partial^2\varphi}{\partial y\partial z}+\frac{\partial^3\psi}{\partial y\partial z^2})-\rho\frac{\partial^3\psi}{\partial y\partial t^2} \tag{6b}$$

$$(\lambda+2\mu)\sigma_{zz}=\lambda\rho\frac{\partial^2\varphi}{\partial t^2}+2\mu(\lambda+2\mu)\cdot(\frac{\partial^2\varphi}{\partial z^2}+\frac{\partial^3\psi}{\partial z^3})-2\rho(\lambda+2\mu)\frac{\partial^3\psi}{\partial z\partial t^2} \tag{6c}$$

3 Forming Potentials

The partial differential equations (Eqs. 5) are transformed from time domain to frequency domain through Fourier transformation method. The potentials in time domain equations are anticipated as conventional exponential scattered wavefields with the form of $e^{-ik_rx}e^{-ik_my}e^{-ik_zz}e^{i\omega_nt}$. In this exponential form, k_r, k_m and k_z are the wavenumbers in three dimensions of x, y and z, respectively. ω_n is the discrete angular frequency. By the method of the separation of variables, the potentials are separated into three independent parts including components x, y and z. The potentials become

$$\tilde{\varphi}=\tilde{\varphi}(z)\cdot e^{-ik_rx}\cdot e^{-ik_my} \tag{7a}$$

$$\tilde{\psi}=\tilde{\psi}(z)\cdot e^{-ik_rx}\cdot e^{-ik_my} \tag{7b}$$

Then the potentials φ and ψ in frequency domain are represented as $\tilde{\varphi}$ and $\tilde{\psi}$. The time factor $e^{i\omega_nt}$ is omitted in the preceding Fourier transforms. When taking Eqs. 7 into the government equation Eqs. 5, one obtains:

$$\frac{\partial\tilde{\varphi}}{\partial x}=-ik_r\tilde{\varphi},\quad \frac{\partial\tilde{\varphi}}{\partial y}=-ik_m\tilde{\varphi} \tag{8}$$

and

$$\frac{\partial^2\tilde{\varphi}}{\partial z^2}+(\frac{\omega_n^2}{C_p^2}-k_r^2-k_m^2)\tilde{\varphi}=0 \tag{9a}$$

$$\frac{\partial^2\tilde{\psi}}{\partial z^2}+(\frac{\omega_n^2}{C_s^2}-k_r^2-k_m^2)\tilde{\psi}=0 \tag{9b}$$

k_{zp} and k_{zs} are related to dilatational (P) waves and shear (S) waves,

$$k_{zp}=(\frac{\omega_n^2}{C_p^2}-k_r^2-k_m^2)^{1/2} \tag{10a}$$

$$k_{zs}=(\frac{\omega_n^2}{C_s^2}-k_r^2-k_m^2)^{1/2} \tag{10b}$$

$k_r$and k_m are independent variables defined by the roots of the plates.

$$k_r=\frac{\pi\cdot r}{l_x},\quad k_m=\frac{\pi\cdot m}{l_y}\quad (r,m=0,1,2...\infty) \tag{11}$$

$l_x$and l_y (Fig.1) represent the lengths from the center to x and y side of plate, respectively.

Substituting Eqs. 8 into Eqs. 4, the displacements obtain

$$\tilde{u}=-ik_r\tilde{\varphi}(z)-ik_r\frac{\partial\tilde{\psi}(z)}{\partial z} \tag{12a}$$

$$\tilde{v}=-ik_m\tilde{\varphi}(z)-ik_m\frac{\partial\tilde{\psi}(z)}{\partial z} \tag{12b}$$

$$\tilde{w}=\frac{\partial\tilde{\varphi}(z)}{\partial z}+\frac{\partial^2\tilde{\psi}(z)}{\partial z^2}+\frac{\omega_n^2}{C_s^2}\tilde{\psi}(z) \tag{12c}$$

Taking Eqs. 8 into Eqs. 6, the stresses are expressed as

$$\tilde{\sigma}_{zx}=-2\mu\cdot i\cdot k_r(\frac{\partial\tilde{\varphi}(z)}{\partial z}+\frac{\partial^2\tilde{\psi}(z)}{\partial z^2}) -\rho\cdot i\cdot k_r\omega_n^2\tilde{\psi}(z) \tag{13a}$$

$$\tilde{\sigma}_{zy}=-2\mu\cdot i\cdot k_m(\frac{\partial\tilde{\varphi}(z)}{\partial z}+\frac{\partial^2\tilde{\psi}(z)}{\partial z^2}) -\rho\cdot i\cdot k_m\omega_n^2\tilde{\psi}(z) \tag{13b}$$

$$\tilde{\sigma}_{zz}=-\frac{\lambda}{C_p^2}\omega^2\tilde{\varphi}(z)+2\mu(\frac{\partial^2\tilde{\varphi}(z)}{\partial z^2} +\frac{\partial^3\tilde{\psi}(z)}{\partial z^3})+2\rho\omega_n^2\frac{\partial\tilde{\psi}(z)}{\partial z} \tag{13c}$$

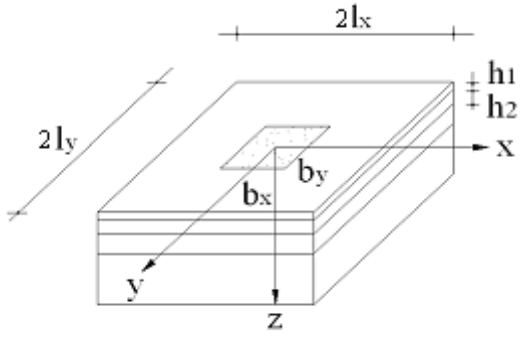

Figure 1 : Structure of 3D layer pavement system

4 Spectral element formulation

The spectral analysis is introduced to solve the problems of 3D layer pavement system(Fig. 1). According to the principle of spectral element analysis (Doyle, 1997), the kernel $\tilde{\varphi}(z,k_r,k_m,\omega_n)$ and $\tilde{\psi}(z,k_r,k_m,\omega_n)$ are the functions of the wavenumbers with three indices of *r*,*m* and *n*. The summation over discrete frequencies is achieved by fast Fourier transformation method (FFT) (Brigham, 1988). $k_r$and k_m are corresponding to the rth and mth vibration modes, respectively.

$$\varphi(x,y,z)=\sum_n\sum_m\sum_r\tilde{\varphi}\cdot e^{-ik_rx}\cdot e^{-ik_my}\cdot e^{i\omega_nt} \tag{14a}$$

$$\psi(x,y,z)=\sum_n\sum_m\sum_r\tilde{\psi}\cdot e^{-ik_rx}\cdot e^{-ik_my}\cdot e^{i\omega_nt} \tag{14b}$$

Substituting the exponential form $A\cdot e^{-ik_{zp}z}$and $C\cdot e^{-ik_{zs}z}$ into $\tilde{\varphi}(z)$ and $\tilde{\psi}(z)$, the potentials in frequency domain become

$$\tilde{\varphi}(x,y,z)=A\cdot e^{-ik_{zp}z}\cdot e^{-ik_rx}\cdot e^{-ik_my} \tag{15a}$$

$$\tilde{\psi}(x,y,z)=C\cdot e^{-ik_{zs}z}\cdot e^{-ik_rx}\cdot e^{-ik_my} \tag{15b}$$

Here *A* and *C* are the coefficients.

4.1 Two-node layer spectral element

Each layer with two bounded interfaces is treated as a two-node layer spectral element(Fig. 2) in which a couple of nodes are located in the centers of surface and bottom, respectively. In the multi-layer system, the bottom note of one layer and the surface note of the neighboring layer are jointed together and numbered as one note in the overall layer structure. Each note has three degrees

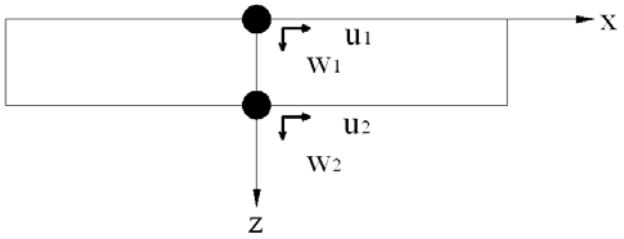

Figure 2 : Two-node layer spectral element

of freedoms in x, y and z directions. Due to the limited depth of z direction in the two-node layer element, the vertical response of wave at any note can be considered as the superposition of the incident wave and the reflection wave. Applying the superposition method, the potentials $\tilde{\varphi}(x,y,z)$ and $\tilde{\psi}(x,y,z)$ in the two-node layer element is the summation of the potentials in the positive z direction and those in negative z directions,

$$\tilde{\varphi}(x,y,z) = (A\cdot e^{-ik_{zp}z} + B\cdot e^{-ik_{zp}(h-z)})\cdot e^{-ik_r x}\cdot e^{-ik_m y} \tag{16a}$$

$$\tilde{\psi}(x,y,z) = (C\cdot e^{-ik_{zs}z} + D\cdot e^{-ik_{zs}(h-z)})\cdot e^{-ik_r x}\cdot e^{-ik_m y} \tag{16b}$$

In these two equations, the first terms in the brackets represent the incident wave propagating from the upper surface at z = 0 and the second terms represent the reflection wave propagating from the boundary at z = h, where h is the thickness of the layer element.

Substituting the potential equations Eqs.16 into the displacement equations Eqs. 12, the x horizontal displacements and the z vertical displacements can be obtained as

$$\tilde{u}_j(x,y,z) = \begin{pmatrix} -A\cdot i\cdot k_r\cdot e^{-i\cdot k_{zp}\cdot z} \\ -i\cdot B\cdot k_r\cdot e^{-i\cdot k_{zp}\cdot(h-z)} \\ -C\cdot k_r\cdot k_{zs}\cdot e^{-i\cdot k_{zs}z} \\ +D\cdot k_r\cdot k_{zs}\cdot e^{-i\cdot k_{zs}(h-z)} \end{pmatrix}\cdot e^{-ik_r x}\cdot e^{-ik_m y} \tag{17a}$$

$$\tilde{w}_j(x,y,z) = \begin{pmatrix} -A\cdot i\cdot k_{zp}\cdot e^{-i\cdot k_{zp}z} \\ +B\cdot i\cdot k_{zp}\cdot e^{-i\cdot k_{zp}(h-z)} \\ C\cdot k^2\cdot e^{-i\cdot k_{zs}\cdot z} \\ +D\cdot k^2\cdot e^{-i\cdot k_{zs}(h-z)} \end{pmatrix}\cdot e^{-ik_r x}\cdot e^{-ik_m y} \tag{17b}$$

in which

$$k = \sqrt{k_r^2 + k_m^2}$$

Each displacement equation consists of coefficients A, B, C and D. The subscription j in $u_j(x,y,z)$ and $w_j(x,y,z)$ denotes the number of notes in the overall layer structure. When taking the conditions of $z = 0$ at note 1 and $z = h$ at note 2 into Eqs. 17, the vector of x and z displacements of each node $[\tilde{u}_1, \tilde{w}_1, \tilde{u}_2, \tilde{w}_2]$ is linked with coefficients A_{mn}, B_{mn}, C_{mn}, D_{mn}in the non-linear equation as follows:

$$\begin{Bmatrix} \tilde{u}_1 \\ \tilde{w}_1 \\ \tilde{u}_2 \\ \tilde{w}_2 \end{Bmatrix} = \begin{bmatrix} -ik_r & -ik_r e_1 & -k_r k_{zs} & k_r k_{zs} e_2 \\ -ik_{zp} & ik_{zp} e_1 & k^2 & k^2 e_2 \\ -ik_r e_1 & -ik_r & -k_r k_{zs}\cdot e_2 & k_r k_{zs} \\ -ik_{zp} e_1 & ik_{zp} & k^2 e_2 & k^2 \end{bmatrix}\cdot \begin{Bmatrix} A \\ B \\ C \\ D \end{Bmatrix} \tag{18}$$

Here $e_1 = e^{-ik_{zp}h}$, $e_2 = e^{-ik_{zs}h}$. The matrix style of Eq.18 is expressed as

$$\tilde{u} = \tilde{N}\cdot\tilde{a} \tag{19}$$

where $\tilde{u}$ represents the nodal displacement vector, $\tilde{a}$ represents the coefficient vector and $\tilde{N}$ is the square matrix. When taking the inverse calculation, Eq. 19 becomes

$$\tilde{a} = \frac{\tilde{M}}{\Delta}\cdot\tilde{u} \tag{20}$$

where the square matrix is defined as $\tilde{N}^{-1} = \tilde{M}/\Delta$. Δ is the determinant of the matrix $\tilde{N}$. Substituting Eqs. 16 into the stress equations (Eqs. 13), the stresses σ_{xz} and σ_{zz} become

$$\sigma_{xzj}(x,y,z) = \begin{pmatrix} 2\cdot A\cdot k_r\cdot k_{zp}\cdot e^{-i\cdot k_{zp}z} \\ -2\cdot B\cdot k_r\cdot k_{zp}\cdot e^{-i\cdot k_{zp}(h-z)} \\ -i\cdot C\cdot R\cdot k_r\cdot e^{-i\cdot k_{zs}z} \\ -i\cdot D\cdot R\cdot k_r\cdot e^{-i\cdot k_{zs}(h-z)} \end{pmatrix} \cdot e^{-ik_r x}\cdot e^{-ik_m y} \tag{21a}$$

$$\sigma_{zzj}(x,y,z) = \begin{pmatrix} A\cdot R\cdot e^{-i\cdot k_{zp}z} \\ +B\cdot R\cdot e^{-i\cdot k_{zp}(h-z)} \\ 2\cdot i\cdot C\cdot k^2\cdot k_{zs}\cdot e^{-i\cdot k_{zs}z} \\ -2\cdot i\cdot D\cdot k^2\cdot k_{zs}\cdot e^{-i\cdot k_{zs}(h-z)} \end{pmatrix} \cdot e^{-ik_r x}\cdot e^{-ik_m y} \tag{21b}$$

where

$$R = \frac{\omega^2}{c_s^2} - 2 \cdot k^2$$

Following the Cauchy stress principle, the tractions on the two nodes of the element surfaces $\tilde{T}_{x1}$, $\tilde{T}_{z1}$, $\tilde{T}_{x2}$ and $\tilde{T}_{z2}$ are corresponding to the normal and shear stresses $\tilde{\sigma}_{xz1}$, $\tilde{\sigma}_{zz1}$, $\tilde{\sigma}_{xz2}$ and $\tilde{\sigma}_{zz2}$, respectively

$$\tilde{T}_{x1} = -\tilde{\sigma}_{xz1}, \quad T_{z1} = -\tilde{\sigma}_{zz1} \tag{22a}$$

$$\tilde{T}_{x2} = \tilde{\sigma}_{xz2}, \quad T_{z2} = \tilde{\sigma}_{zz2} \tag{22b}$$

The stresses T_{x1}, T_{x2}, T_{z1} and T_{z2} in each layer are derived by taking Eqs.21 to Eqs.22. In the same way of displacement equations, they become

$$\begin{Bmatrix} T_{x1} \\ T_{z1} \\ T_{x2} \\ T_{z2} \end{Bmatrix} = \mu \cdot \begin{bmatrix} 2k_r k_{zp} & -2k_r k_{zp} e_1 \\ R & R \cdot e_1 \\ -2 \cdot k_r k_{zp} e_1 & 2k_r k_{zp} \\ -R \cdot e_1 & -R \\ -iRk_r & -iRk_r e_2 \\ 2ik^2 k_{zs} & -2ik^2 k_{zs} e_2 \\ iRk_r e_2 & iRk_r \\ -2ik^2 k_{zs} e_2 & 2ik^2 k_{zs} \end{bmatrix} \cdot \begin{Bmatrix} A \\ B \\ C \\ D \end{Bmatrix} \tag{23}$$

It can be written as

$$\tilde{T} = \mu \cdot \tilde{P} \cdot \tilde{a} = \mu \cdot \frac{\tilde{P} \cdot \tilde{M}}{\Delta} \cdot \tilde{u} = (\mu/\Delta) \cdot \tilde{k} \cdot \tilde{u} \tag{24}$$

Here $\tilde{k} = \tilde{P} \cdot \tilde{M}$. Neglecting of the skew tensors, $\tilde{k}$ is a complex and symmetric 8×8 matrix corresponding to the dynamic element stiffness in the conventional finite element method.

$$\tilde{k} = \begin{bmatrix} k_{11} & k_{12} & k_{13} & k_{14} \\ & k_{22} & -k_{14} & k_{24} \\ & & k_{11} & -k_{12} \\ & & & k_{22} \end{bmatrix} \tag{25}$$

4.2 One-node throw-off spectral element

The one-node throw-off spectral element(Fig. 3) is a semi-infinite element. It assumed that wave propagates only in the positive z direction. Due to the absence of reflection wave in the throw-off element, the potentials of dilatational and shear waves can be simplified by equalizing the coefficients B and D zero. Therefore, the potentials of this element have the same expression as Eqs. 15, and the displacements are obtained as

$$\tilde{u}_j = (-A \cdot i \cdot k_r \cdot e^{-i \cdot k_{zp} \cdot z} - C \cdot k_r \cdot k_s \cdot e^{-i \cdot k_{zs} z}) \cdot e^{-ik_r x} \cdot e^{-ik_m y} \tag{26a}$$

$$\tilde{w}_j = (-A \cdot i \cdot k_p \cdot e^{-i \cdot k_{zp} z} + C \cdot k^2 \cdot e^{-i \cdot k_{zs} \cdot z}) \cdot e^{-ik_r x} \cdot e^{-ik_m y} \tag{26b}$$

Coefficients A and C are derived from Eqs. 26. That is

$$\begin{Bmatrix} A \\ C \end{Bmatrix} = (1/\Delta) \begin{bmatrix} ik^2/k_r & ik_{zs} \\ -k_{zp}/k_r & 1 \end{bmatrix} \begin{Bmatrix} \tilde{u} \\ \tilde{w} \end{Bmatrix} \tag{27}$$

where $\Delta = k^2 + k_{zp} k_s$

Following the Cauchy stress principle, the tractions of the node are related to the stresses by

$$\tilde{T}_{x1} = -\tilde{\sigma}_{xz}, \quad \tilde{T}_{z1} = -\tilde{\sigma}_{zz} \tag{28}$$

Substituting Eqs. 15 into the stress equations Eqs. 13 and Eq. 28, the stresses $\tilde{T}_{x1}$ and $\tilde{T}_{z1}$ can be expressed as

$$\begin{Bmatrix} \tilde{T}_{x1} \\ \tilde{T}_{z1} \end{Bmatrix} = \mu \begin{bmatrix} 2k_r k_{zp} & -iRk_r \\ R & 2ik^2 k_{zs} \end{bmatrix} \begin{Bmatrix} A \\ B \end{Bmatrix} \tag{29}$$

In the similar way of the two-node element, the stresses become

$$\begin{Bmatrix} \tilde{T}_{x1} \\ \tilde{T}_{z1} \end{Bmatrix} = (\mu/\Delta) \begin{bmatrix} k_{11} & k_{12} \\ k_{21} & k_{22} \end{bmatrix} \begin{Bmatrix} \tilde{u} \\ \tilde{w} \end{Bmatrix} \tag{30}$$

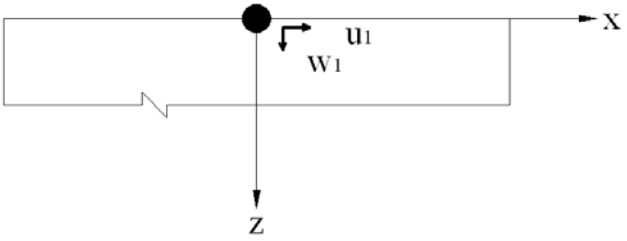

Figure 3 : One-node throw-off spectral element

5 Assemblage of the global stiffness matrix and spectral structure

Under the condition that the displacements are compatible between two elements, the global stiffness matrix is assembled by the layer elements and one throw-off element. The rule of assemblage is similar to the conventional finite element method.

The global equation is expressed as:

$$\left[\tilde{K}(z,k_r,k_m,\omega_n)\right]\cdot\tilde{U}=\tilde{P} \tag{31}$$

$\left[\tilde{K}(z,k_r,k_m,\omega_n)\right]$, the global stiffness matrix, is a symmetric complex and banded matrix. $\tilde{U}$ is the global displacement vector, and $\tilde{P}$ is the global force vector. These two vectors in frequency domain can be evaluated by the displacement and stress boundary conditions. The relationship between the forces $\tilde{P}$ and tractions $\tilde{T}$ of the neighboring two layer elements is:

$$\tilde{P}_{xi}=A\times\left(\tilde{T}_{x2}^{i-1}+\tilde{T}_{x1}^{i}\right),\quad \tilde{P}_{zi}=A\times\left(\tilde{T}_{z2}^{i-1}+\tilde{T}_{z1}^{i}\right) \tag{32}$$

Here A is the area of the applied load. At the surface node, that relationship above becomes

$$\tilde{P}_{xi}=A\times\tilde{T}_{x1}^{i}\quad,\quad \tilde{P}_{zi}=A\times\tilde{T}_{z1}^{i} \tag{33}$$

Following the expression of Eqs. 14, the in-time displacement at nodes can be displayed as follows:

$$u_i=\sum_n\sum_m\sum_r\tilde{G}\cdot\tilde{P}\cdot\tilde{F}_{rm}\cdot e^{-ik_rx}\cdot e^{-ik_my}\cdot\tilde{F}_n\cdot e^{i\omega_nt} \tag{34}$$

$\tilde{G}$ is the inverse matrix of $\left[\tilde{K}(z,k_r,k_m,\omega_n)\right]$. If $\tilde{P}$ only includes the vertical displacement at the first node in the whole layer structure, $\tilde{P}$ will become a unit vector. Then the in-time displacement becomes:

$$u_i=\sum_n\sum_m\sum_r\tilde{u}_i\cdot\tilde{F}_{rm}\cdot e^{-ik_rx}\cdot e^{-ik_my}\cdot\tilde{F}_n\cdot e^{i\omega_nt} \tag{35}$$

Here $\tilde{u}_i$ is displacement vector calculated in the frequency domain. The in-time displacement is achieved by a double summation over the wavenumbers and Fourier transforms over the angular frequencies. $\tilde{F}_{rm}$ is the coefficient of the spatial distribution of the applied load. And $\tilde{F}_n$ is the time variation coefficient that is determined by the theory of Fast Fourier Transformation (FFT).

5.1 Determination of $\tilde{F}_{rm}$

FWD load function can be separated into two independent parts,

$$P[(x,y),t]\quad=f(x,y)\cdot\quad F(t). \tag{36}$$

$f(x,y)$ is the spatial distribution function of the cubic shape load and $F(t)$ is the time variation function. If FWD applied load is a cylindrical shape load, an equivalent cubic shape load can be assumed with rectangular $2b\times 2b$ and amplitude q, which is

$$f(x,y)=\begin{cases} q & for -b\le x\le b,-b\le y\le b \\ 0 & another \end{cases} \tag{37}$$

The spatial distribution of the applied load $f(x,y)$ can be separated into two independent variables, $f(x)$ and $f(y)$, shown as

$$f(x)=\sum_r a_r(x)\cdot\cos(k_rx) \tag{38a}$$

$$f(y)=\sum_m a_m(y)\cdot\cos(k_my) \tag{38b}$$

Here, the coefficients of Fourier series are

$$a_{r,m}(s)=\begin{cases} \frac{1}{l_s}\int_0^{l_s}f(s)\cos(k_{r,m}s)ds & r,m=0 \\ \frac{2}{l_s}\int_0^{l_s}f(s)\cos(k_{r,m}s)ds & another \end{cases}, \tag{39}$$

Eq. 39 shows the results of $a_r(x)$ and $a_m(y)$. And s denotes the coordinates x or y. Then, the method of double Fourier transformation is utilized to determinate the spatial distribution coefficient $\tilde{F}_{rm}$.

$$\begin{aligned} f(x,y)&=f(x)\cdot f(y)\\ &=\sum_r\sum_m a_r(x)a_m(y)\cos(k_rx)\cos(k_my)\\ &=\sum_r\sum_m\tilde{F}_{rm}\cos(k_rx)\cos(k_my)\\ \text{and,}\quad \tilde{F}_{rm}&=a_r(x)a_m(y). \end{aligned} \tag{40}$$

6 Numerical Verification

The above-formulated three-dimensional layer spectral element program(3DSEP) is evaluated through comparing the calculated results with those of a 3D finite element method program and the axi-symmetric spectral element program(LAMDA) developed by AL-Khoury.

Table 1 : Geometrical and material properties

	Thickness (mm)	E (MPa)	Poisson's ratio	Mass density (kg/m^3)
Asphalt	150	1000	0.35	2300
Subbase	250	200	0.35	2000
Subgrade	15000	100	0.35	1500

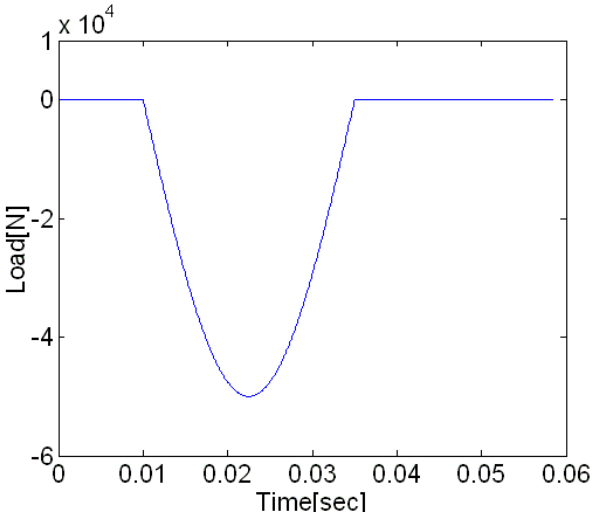

Figure 4 : Load pulse of FWD

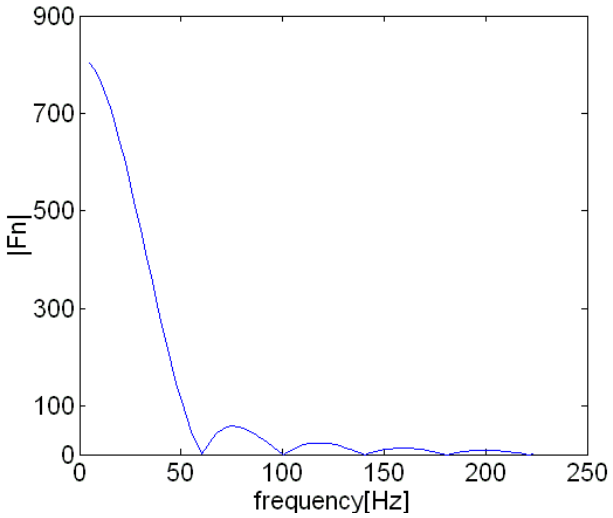

Figure 5 : Frequency spectrum

A pavement is subjected to a vertical load pulse that is distributed uniformly within a square of 133 $\times$ 133mm^2. The time history of the load pulse and its frequency spectrum are displayed in Fig. 4 and Fig. 5.

Three-dimensional finite element program CAPA-3D (Scarpas, 1993) is implemented for the computational analysis of the pavement structure displayed in Fig. 6, which is composed of three typical layers asphalt, subbase and subgrade. The properties of the pavement materials are presented in Tab.1. Finite element meshes of the pavement model are represented in Fig. 6. The upper two layers, asphalt and subbase, have a surface area of $6m \times 6m$. The subgrade as soil foundation has a larger surface area of $20m \times 20m$.

The maximum of iteration coefficients r and m depends on the property of the load pulse and the geometrical magnitudes of the layers. In this case, r and m range from zero to 30. The number of sampling data utilized in FFT was N=2048. For such a load pulse in the example, the analysis to the maximal frequency is 150Hz.

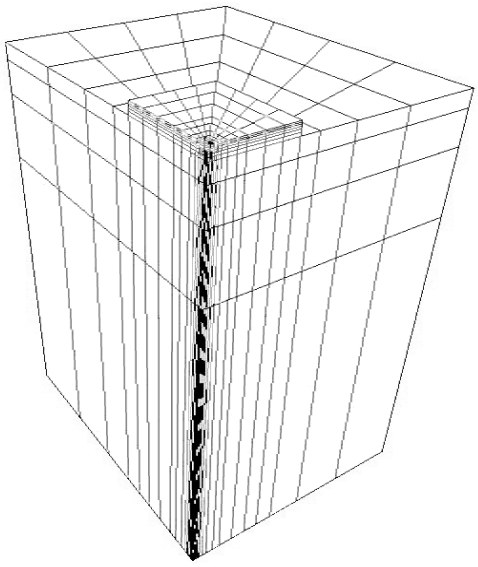

Figure 6 : Finite element meshes of the pavement structure

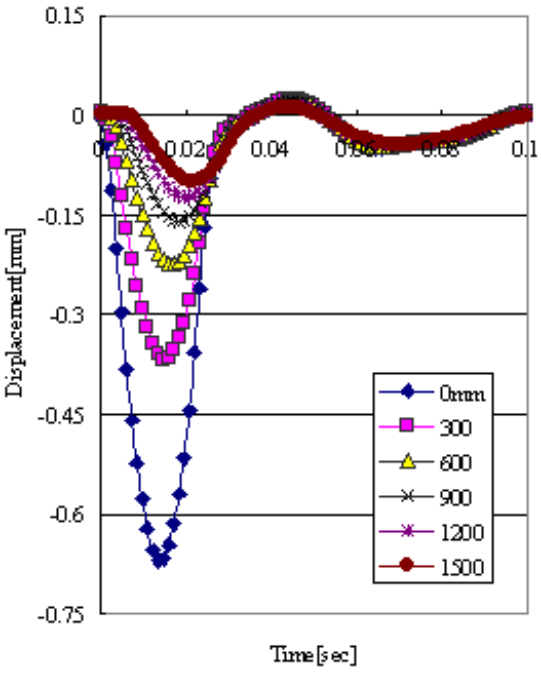

(a) 3DSEP

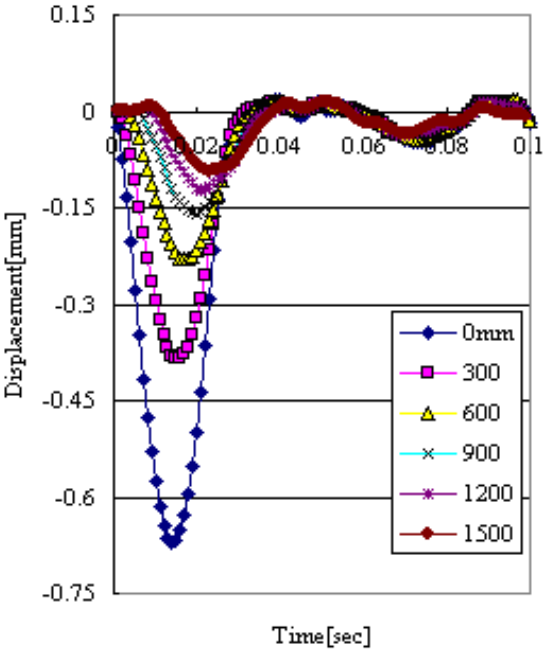

(b) CAPA-3D

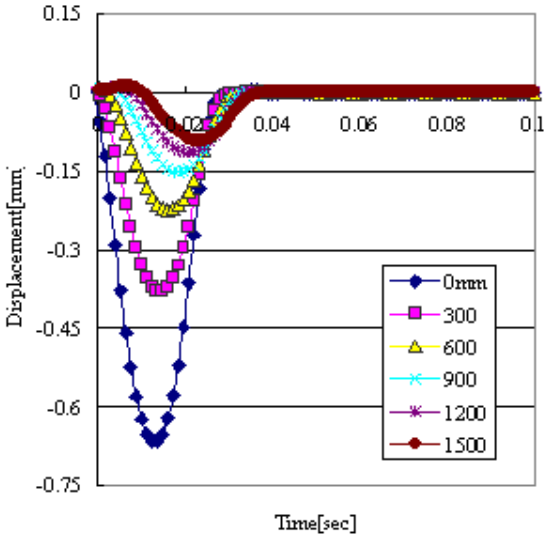

(c) LAMDA

Figure 7 : Results of the numerical example

Three kinds of method were employed to analyze the numerical example. The curves in Fig.7 express vertical displacement at different locations from 0 mm to 1500 mm. The three charts in Fig.7 show that results from three methods are in good agreement at the first pulse that occurs before 0.04 sec. Due to the model of the axi-symmetric infinite layers, the result from program LAMDA has no second pulse. The 3D layer spectral element method and the finite element method can simulate layers with boundaries, so the solutions of Fig. 7(a) and (b) are similar in the whole histories of propagation. However, for a 256MHz Intel PC, the time consumption for 3DSEP Fig. 7(a) was 4 seconds, that for LAMDA Fig. 7(c) was 8 seconds, whereas $1/2$ hour was needed for the 3D finite element method (Fig. 7(c)). It is clear that the 3D layer spectral element method is more efficient than axi-symmetric spectral element program and much more efficient than the 3D finite element program.

7 Conclusions

The three-dimensional layer spectral element is developed in the study for the analysis of multi-layered pavement system subjected to the dynamic load. Based on the spectral analysis, one element is adequate to describe one layer, so the number of the element meshes is equal to the

number of the layers. The system is solved by the multi-summation over the frequencies and the wavenumbers, which alleviates the inconvenience of the numerical calculation of infinite integration. The transformation from time to frequency domain is achieved by using FFT(Fast Fourier transforms), and procedures from frequency to time domain are done by means of IFFT(Inverse FFT).

A numerical example was presented to compare the results from the proposed method in this paper with those from finite element method and axi-symmetric spectral element method(LAMDA). Because of its high efficiency in computation, the 3D layer spectral element approach can be widely used in the backcaculation of FWD test of pavement system.

Acknowledgement: The authors would like to thank Dr. R. Al-Khoury and C. Kasbergen for their cordial help.

References

Al-Khoury, R.; Scarpas, A.; Kasbergen, C.; Blaauwendraad, J. (2001a): Spectral element technique for efficient parameter identification of layered media, Part I: Forward calculation. *International Journal of Solids and Structures* vol. 38, pp. 1605–1623.

Bozkurt, D.(2002): Three dimensional finite element analyses to evaluate reflective cracking potential in asphalt concrete overlays. Thesis for PHD, University of Illinois at Urbana-Champaign.

Brigham, E.O. (1988): The Fast Fourier Transform and Its Applications. Prentice-Hall, Englewood Cli.s, NJ.

Doyle, J.F. (1997): Wave Propagation in Structures: Spectral Analysis using Fast Discrete Fourier Transforms. Springer-Verlag, New York.

Haskell, N.A.(1953):The dispersion of surface waves on multilayered media. *Bull. Seism. Soc. Am.* vol. 43, pp.17-34.

Kausel, E.; Roesset, J.M. (1981): Stiffness matrices for layered soils. *Bull. Seism. Soc. Am.* vol.71, pp.1743-1761.

Kim, Y. (1998): Prediction of layer moduli from falling weight deflectometer and surface wave measurements using artificial neural network *Transportation Research Record*, vol. 1639, pp. 53-61

Lamb, H. (1904): On the propagation of tremors over the surface of an elastic solid, *philosophical transactions of royal society*, V. CCIII(1), pp.1-42

Lee, Y.C. ; Kim, Y. R. ; Ranjithan, S. R. (1998): Dynamic analysis-based approach to determine flexible pavement layer moduli using deflection basin parameters. *Transportation Research Record*, vol. 1639, pp. 36-42

Rizzi, S.A.; Doyle, J.F. (1992): Spectral analysis of wave motion in plane solids with boundaries, *Journal of Vibration and Acoustics*, vol. 114, pp.133-140

Rizzi, S.A.; Doyle, J.F. (1992) : A spectral element approach to wave motion in layered solids, *Journal of Vibration and Acoustics*, vol. 114, pp. 569-577

Thomson, W.T. (1950): Transmission of elastic waves through a stratified solid media. *J. Applied Phys*, vol. 21, pp. 89-93.

Scarpas, A. (1993). CAPA-3D Finite Elements System-User's Manual Parts , and . Section of Structural Mechanics, Faculty of Civil Engineering and Geosciences, TU-Delft, The Netherlands.